

Exploration of Asymmetric Ligament Behaviours of Lower Leg Injury in Automotive Pedestrian Impact

Ben Crone¹, Jean Bout¹,

¹Arup (Specialist Technologies Analytics and Research), Birmingham, UK

Abstract

During physical testing for UN ECE R127 lower leg impact on a sports vehicle, a pronounced asymmetry was observed in Flex-PLI PCL knee elongation between impacts on the left and right sides of the vehicle. This paper investigates the potential causes of this asymmetry, examining its sensitivity to variations in vehicle geometry, impact conditions, and pedestrian orientation. Using Ansys LS-DYNA®, simulations are performed across a range of vehicle morphologies and impact configurations, including both leading-leg and trailing-leg scenarios. The study is further extended to aPLI and Human Body Model (HBM) impactors to assess whether similar trends emerge across different impactor types. These investigations aim to highlight considerations for interpreting test outcomes and may inform future discussions around the selection of outboard test locations in regulatory protocols.

Introduction

As part of Arup's consultancy services, the authors were asked to provide insight into an anomalous result recorded during physical testing for UN ECE R127 lower leg impact on a sports vehicle. A pronounced asymmetry was observed in Flex-PLI posterior cruciate ligament (PCL) knee elongation between physical impacts on the left and right extremities of the vehicle, amounting to a >25% difference between PCL elongation when compared to the left-hand side and other RHS repeats (Figure 1). Across these various physical tests, no comparable anomaly was observed for anterior cruciate ligament (ACL) elongation, with the only discernible difference between the anomalous result and other impacts being a small amount of impactor inflight yaw, observable in the test video.

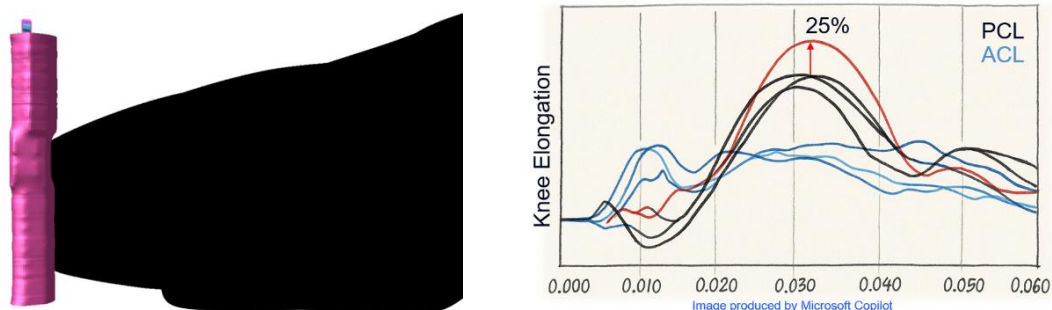


Figure 1 – UN ECE R127 Lower Leg Impact & Illustrative Test Result

Prior to physical testing, CAE predictions (LS-DYNA R11.2.2) had not detected a *significant* difference left to right, with any small differences in injury being attributed to vehicle asymmetry and/or analysis variability.

Numerous CAE studies were conducted to explain the +25% anomalous test result, from which it was concluded that impactor yaw (rotation about the z-axis) was the driver of the high injury, as corroborated by the physical test footage. Furthermore, the studies highlighted that both ACL and PCL were sensitive to how the leg rolled on the vehicle A-surface, and that the sensitivity varied both with impactor yaw as well as the side of the vehicle impacted. Vehicle right-hand side (RHS) typically producing the highest PCL injury.

However, it was not clear whether this injury/leg behaviour was a function of the specific vehicle tested or something more fundamental.

The UN ECE R127 assessment for leg injury utilises the Flex-PLI legform impactor, this impactor representing a 50th percentile male RHS leg, with the direction of the foot pointing towards the vehicle RHS [1]. For a vehicle RHS impact, the leg effectively leads the path of the vehicle, whereas in a left-hand side (LHS) impact, the leg trails behind path of the vehicle.

To confirm that the cause of the anomaly was not due to vehicle asymmetry, Arup conducted a reflected vehicle simulation, where the vehicle model was reflected about the ZX plane. The red lines in Figure 2 show that for both the versions of the vehicle model, PCL injury was consistently greatest on the RHS.

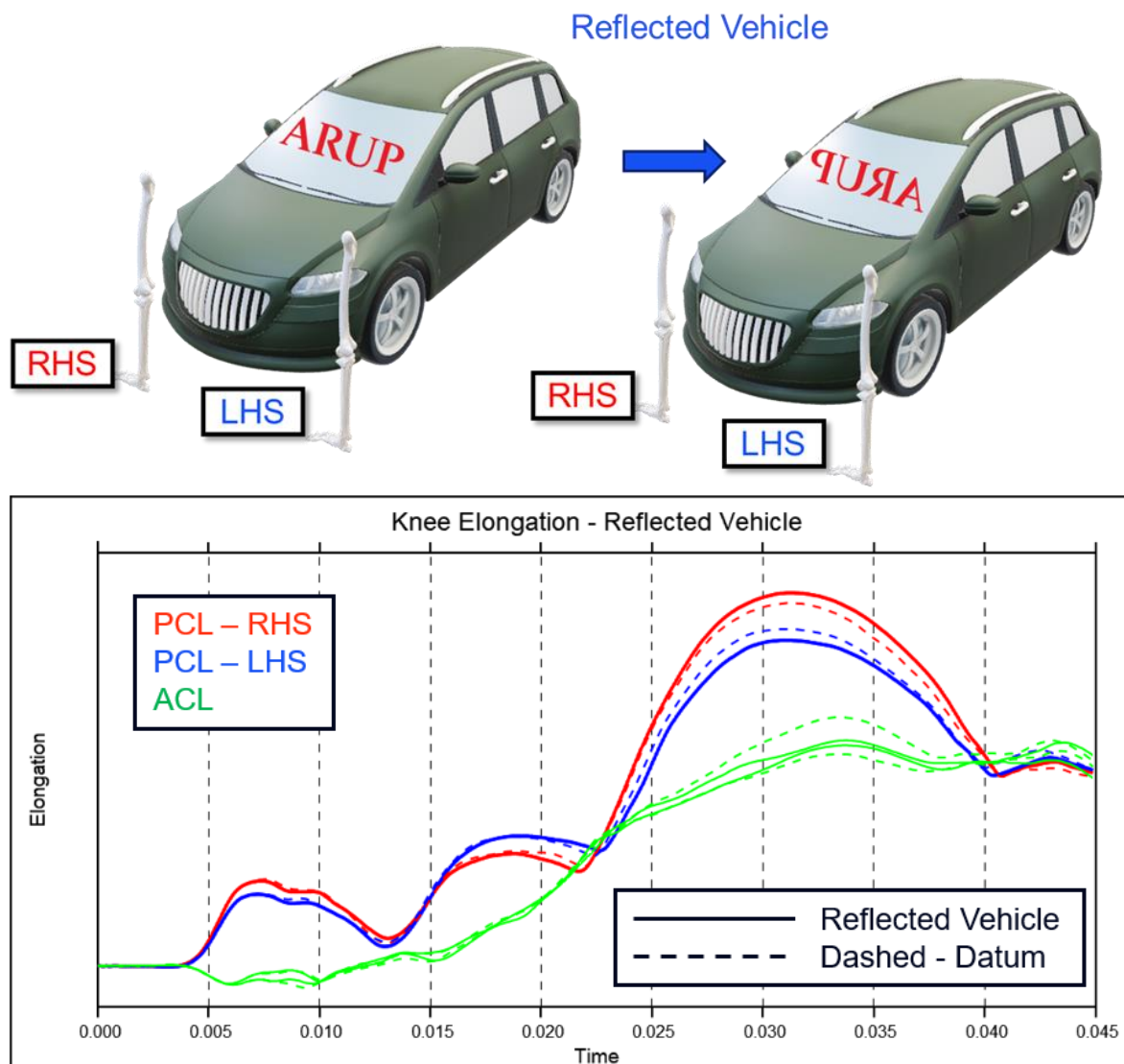


Figure 2 – Reflected Vehicle Study Illustration and Injury results

Additionally, the analysis was also run with impactor reflected, now representing a LHS leg, the foot pointing toward the vehicle LHS. In this case, Figure 3 shows that the LHS became worst-case for PCL when the leg was reflected (blue solid line), compared to the RHS (red line) for the datum

This subsequently confirms that the asymmetry between left and right is reproducible and could be attributed solely to the impactor, rather any vehicle asymmetries.

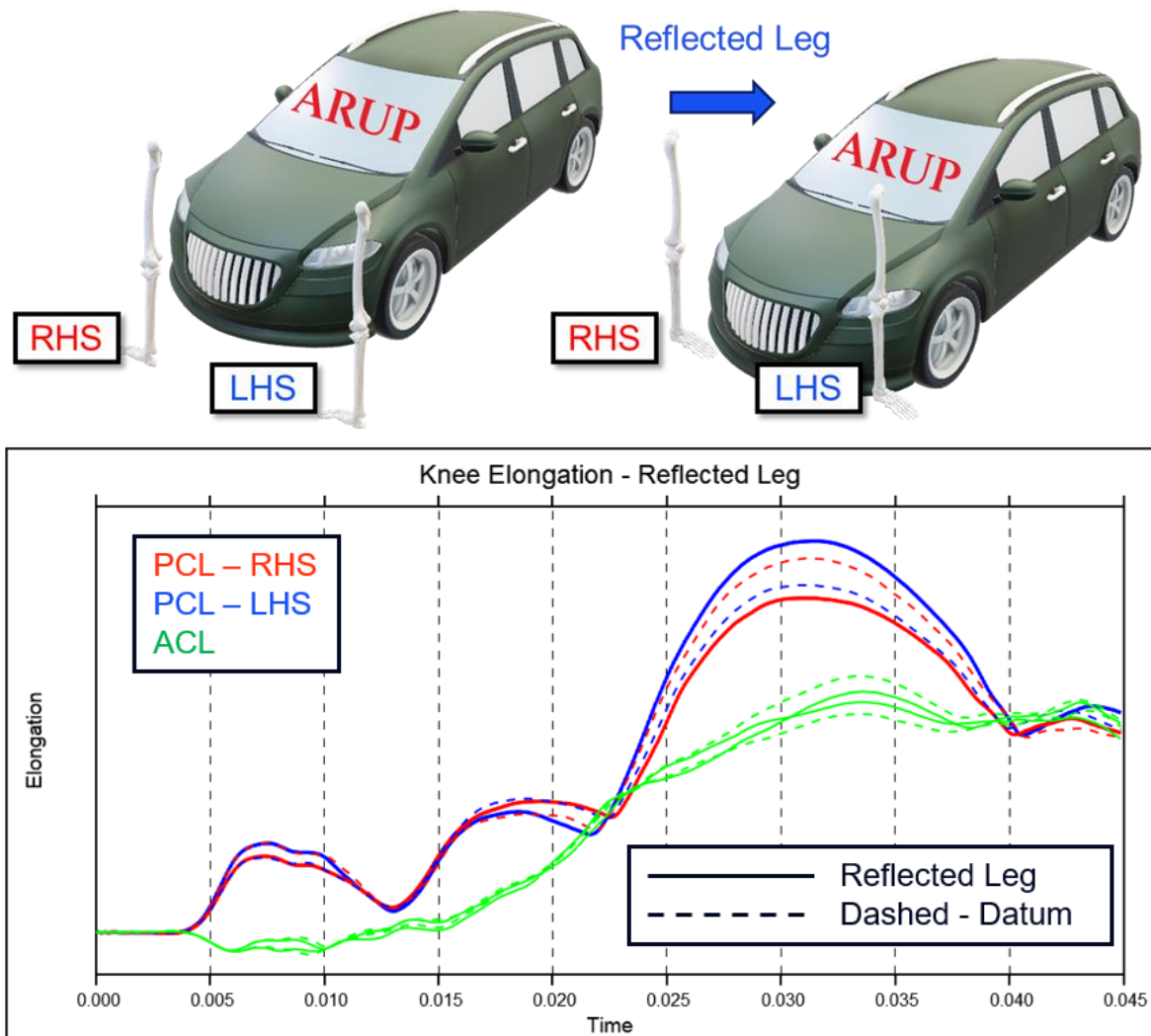


Figure 3 – Reflected Leg Study

Overview of Injury Mechanism

The mechanisms for ligament injury with the Flex-PLI impactor for low bumper vehicles can be attributed around two key events (Figure 4):

- 1) Valgus rotation (away from body centre line) / bending of the legform caused by the unopposed displacement of the upper leg.
- 2) Knee/upper tibia shear, generated by the bumper only loading and interacting with the lower leg.

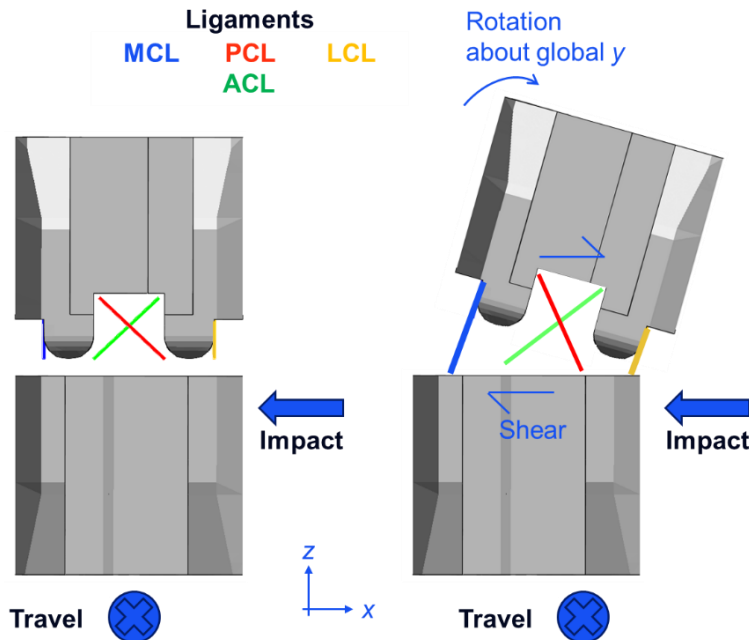


Figure 4 – Posterior view of Flex-PLI knee deformation during impact.

The shearing of the knee compartment drives elongations primarily to the medial cruciate ligament (MCL) and ACL whilst the bending of the legform also compounds any MCL elongation. PCL elongation arises as a function of the relative motion of the upper and lower leg, specifically through any posterior displacement and/or hyperextension of the joint (Figure 5).

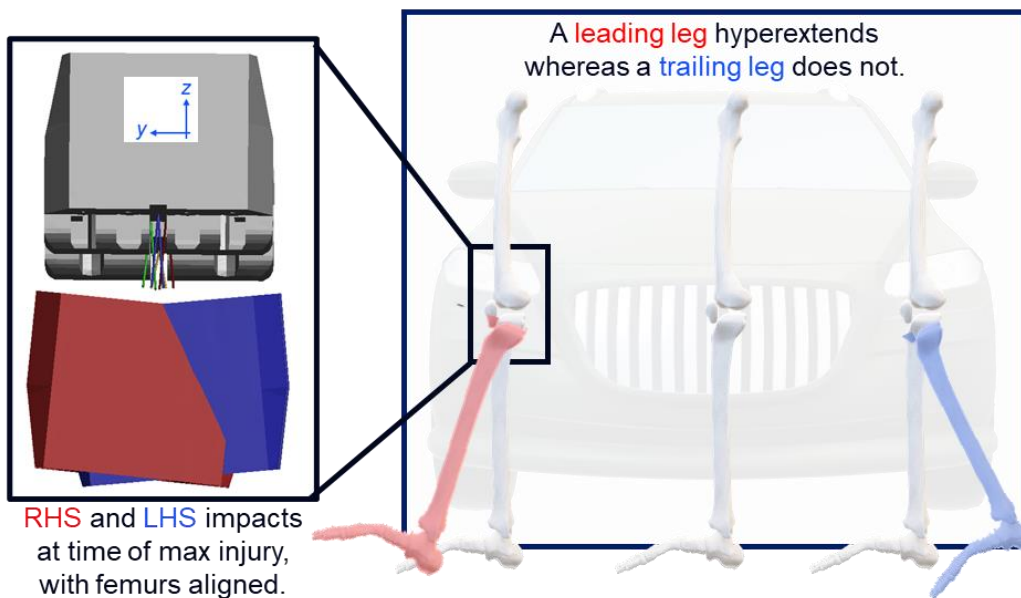


Figure 5 – Sagittal view of leg hyperextension, dependent on which side of oblique impact occurs.

These injury mechanisms further evolve for outboard corner impacts on a vehicle, where the angled A-surface of the vehicle acts to rotate the tibia upon impact. This in turn rotates the upper leg but

importantly not its trajectory. This results in a global rotation of the upper leg about a locally shifted axis, effectively decoupling the legform's rotational behaviour from its translational path. The altered axis of rotation leads to a pronounced hyperextension of the tibia relative to the femur for a RHS impact (Figure 6).

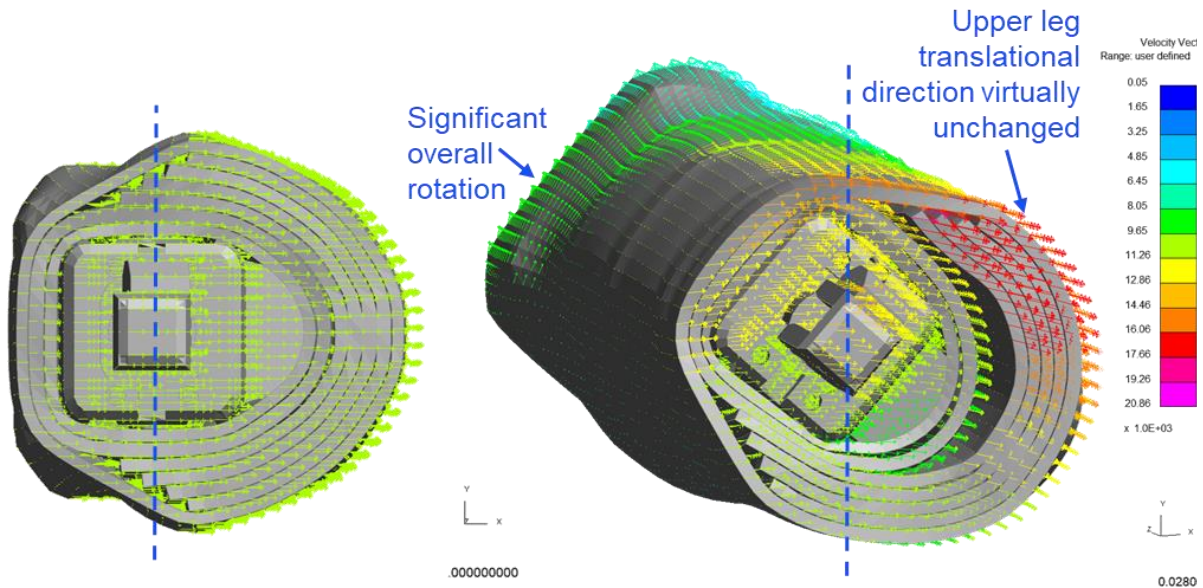


Figure 6 – Velocity vector plot of Flex PLI initial vs collision impact, highlighting rotational behaviour induced by impact onto tibia.

This additional hyperextension, developed by the oblique impact, produces an exaggerated elongation of the PCL when compared to baseline loading conditions. For a RHS impact this additional valgus torsion of the tibia drives the hyperextension of the joint, whereas on the LHS, the opposite direction torsion (varus) on the tibia causes limited influence on PCL for the particular sports vehicle in question.

To further understand this mechanism and importantly identify what sensitivities may bolster this phenomena, a series of studies will be conducted to discern:

1. What vehicle geometries/parameters have influence on producing this asymmetry?
2. What impactor sensitivities that arise from test can influence this behaviour?
3. Are alternate ATD impactors or HBM models subject to the same asymmetric behaviour?

Submodel Development and Validation

To assess the sensitivity of this ligament behaviour across a range of vehicle geometries, a submodel was created based upon qualities of the original vehicle. The submodel, shown in Figure 7, consisted of three regions of rigid shell elements representing the different regions across a vehicle A-surface, a lower, middle and upper bumper.

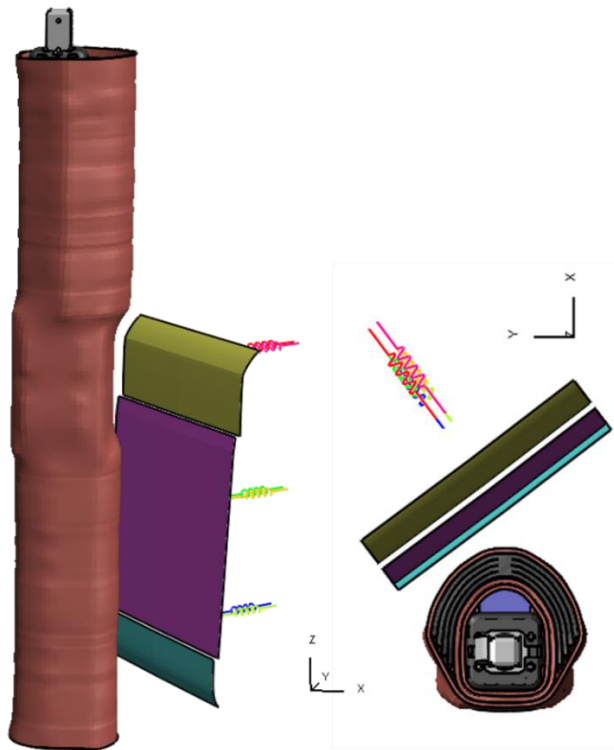


Figure 7 – Vehicle Submodel

Rearwards of each A-surface region, a pair of discrete elements act individually in the global x and y-directions. The shells were constrained such that they could only displace in global x and y-directions. The stiffness of the discrete elements was determined using force and displacement transducer output extracted from the full vehicle model: implemented using **MAT_S04 : SPRING_NONLINEAR_ELASTIC** and one-way curves in x and y-directions, shown in Figure 8, arranged in such a way to prevent excess spring back beyond the nominal A-surface.

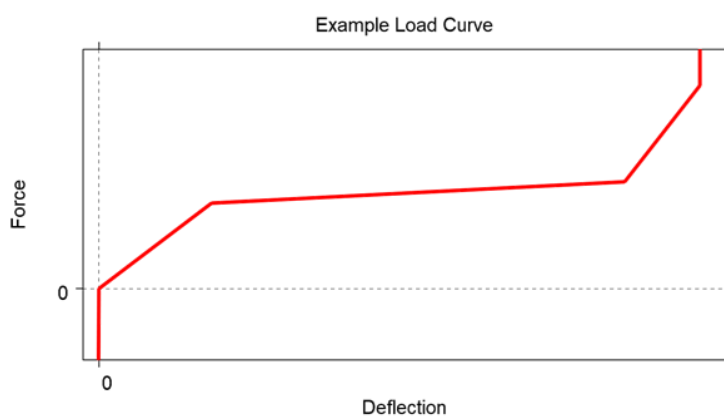


Figure 8 – Example Load Curve for Vehicle Springs

The initial height of the submodel components was approximately 600 mm, (from ground) with a corner angle of ~30 degrees and a nose angle of 20 degrees.

The submodel was subsequently compared to the datum vehicle using the Flex-PLI impactor to validate its performance in delivering reasonably realistic bumper deformation and appropriate ligament elongation.

Reviewing the comparison of injury curves in Figure 9, the submodel demonstrates good agreement between peak MCL elongations for both LHS and RHS, suggesting similar upper leg kinematics to the datum vehicle. The extent of PCL elongation broadly follows the same timing and shape as the full model; however, it is noted that the submodel slightly underpredicts peak PCL injury. ACL injury has good agreement with full model peak injury however the shape of the curve is not exact, with slightly more ramps in elongation before reaching its peak elongation.

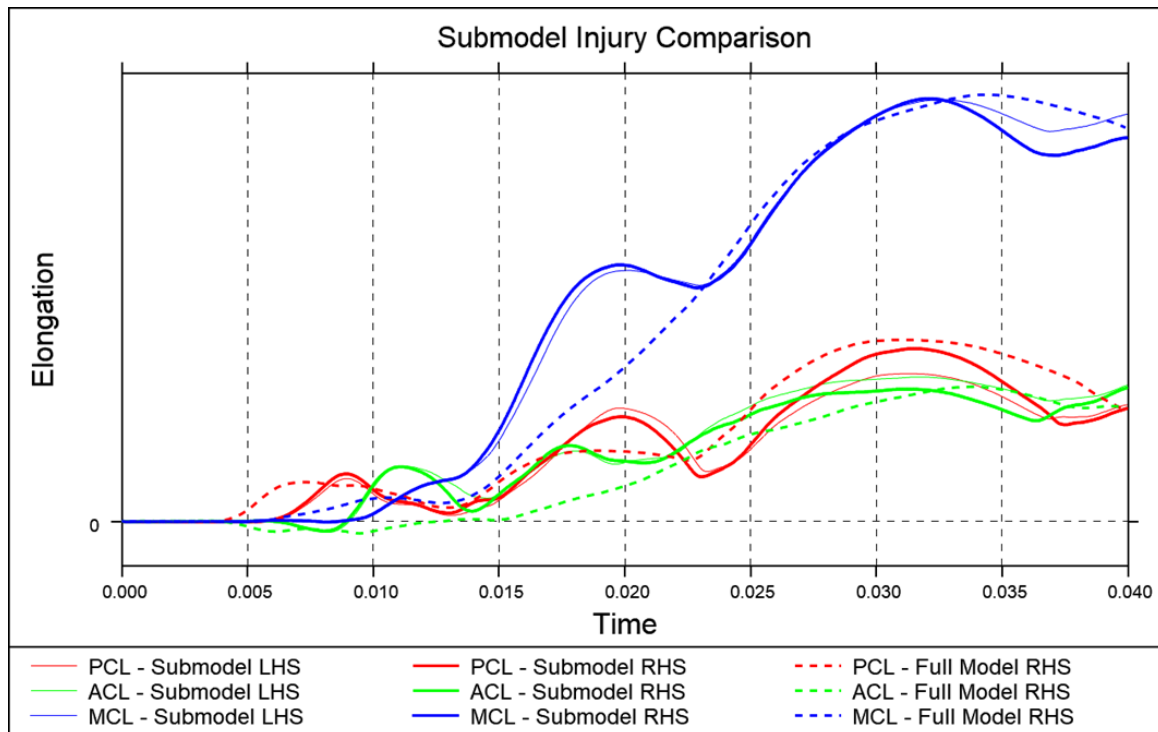


Figure 9 – Comparison of submodel LHS and RHS to full vehicle injury

The submodel also successfully demonstrated the key ligament asymmetry phenomenon for the PCL, with the RHS impact side having a higher elongation than the LHS, the simulation showing the aforementioned hyperextension behaviour as the datum model. To further verify the submodel, a comparison was also made between contact forces, ensuring similar load path distribution across the A-surface regions in both models.

Vehicle Design of Experiments

The aforementioned submodel was subsequently parameterised in order to develop a range of vehicle morphologies that encompass a significant range of vehicles. Parameters selected for investigation are tabulated below in Table 1, the overall design space was defined to represent typical geometries from sports car to SUV.

Table 1 – Overview of Design Space and Parameters

Parameter	Min	Max
Angle	+/- 5	+/- 45
Z Height Scale Factor	1.0*	2.0
Nose Angle	0	60

*Baseline height = ~600mm from ground.

The impactor orientation on the car being LHS or RHS was determined by whether the corner angle of the vehicle was positive or negative, allowing for matching left and right-hand analysis to be conducted for each design permutation of the vehicle. The spread in design space and influence of the parameters on the submodel can be visualised in **Error! Reference source not found.**. A full factorial point selection was used across the design space.

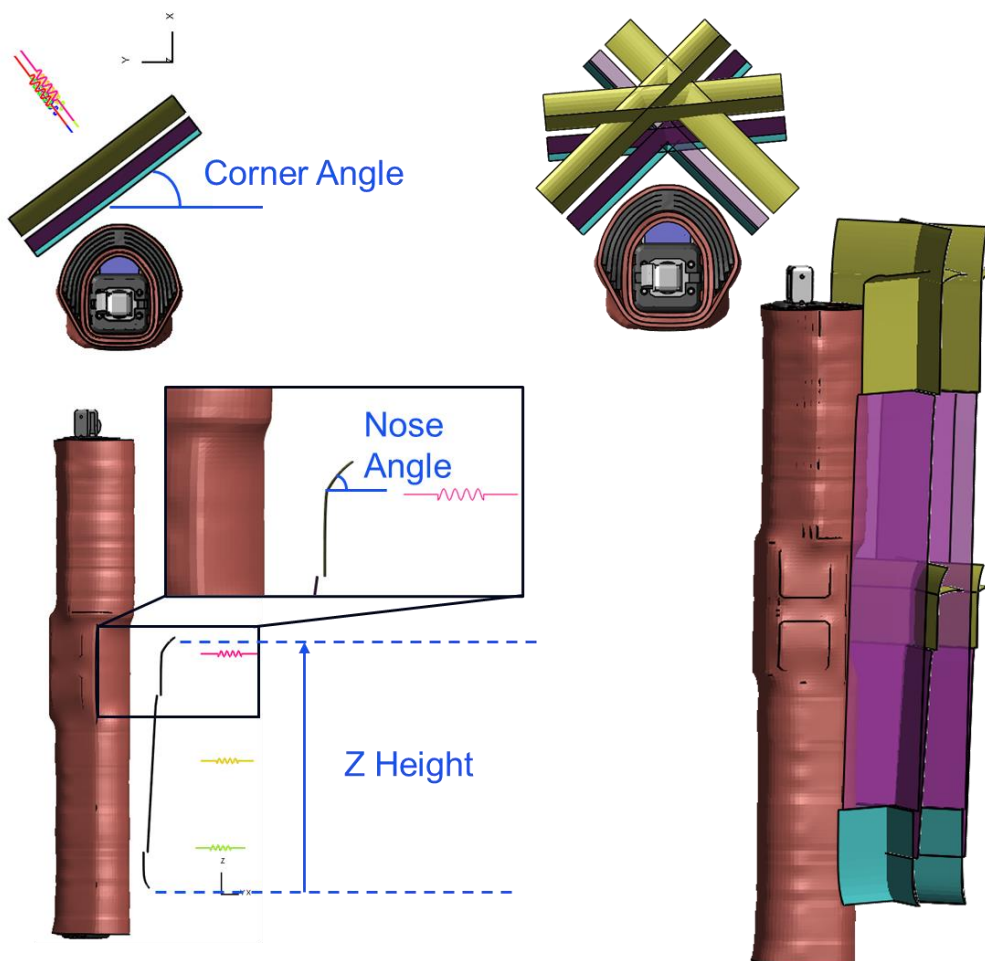


Figure 10 – Example of parameter effects on submodel (LHS). Example of vehicle morphology ranges achieved in design space relative to Flex PLI impactor (RHS).

Nearly 100 pairs of impacts were extracted from the vehicle DoE, with the Oasys LS-DYNA Environment used to post process and extract injury curves. The peak ligament injuries were input into LS-OPT for further post-processing. An initial assessment of the injuries can be seen in Table 2.

Table 2 – Statistical summary of LHS and RHS cruciate ligament injuries

(mm)	LHS Mean	LHS Max	RHS Mean	RHS Max
PCL	8.4	10.1	8.6	11.7
ACL	7.2	12.3	7.0	10.8
MCL	12.0	30.0	12.1	29.8

Reviewing both sides of the vehicle, the RHS analyses demonstrated a bias for higher PCL elongation. Conversely, ACL tended to be worse on the LHS analysis, noting that absolute elongations were on average greater than PCL. Reviewing MCL, it was observed that it was largely insensitive to impact side, consistent with previous findings by Isshiki et al [2].

Using LSOPT, the simulation data was subsequently used in a Feed Forward Neural Network in order to generate an appropriate metamodel of the design space to infer key behaviours (Figure 11).

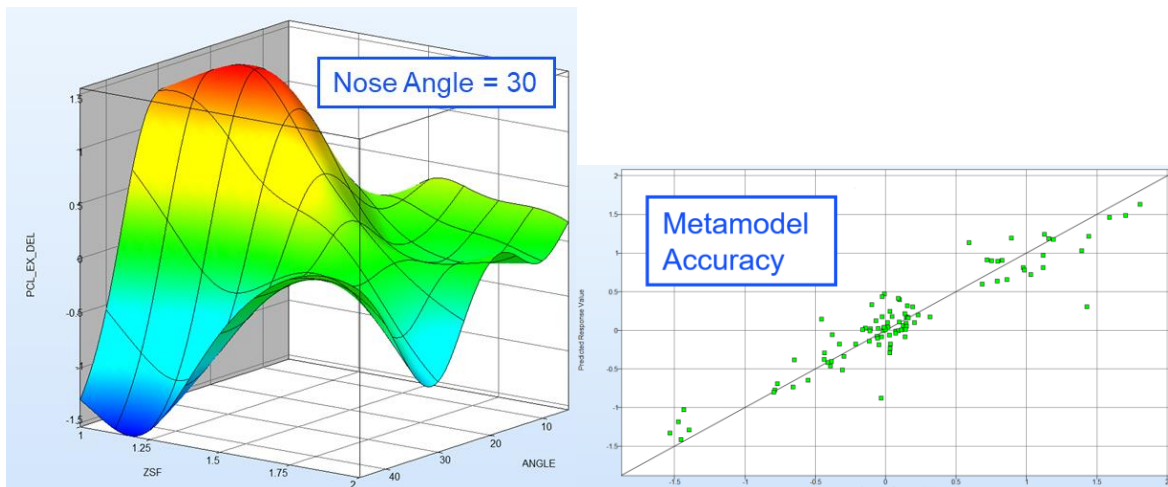


Figure 11 – Example vehicle morphology metamodel, and its accuracy, noting changes in PCL delta (RHS-LHS) with respect to bumper height (ZSF) and Corner Angle (ANGLE) for a nose angle of 30 degrees.

From this metamodel analysis, key findings on parameters of vehicle morphology were found to influence ligament asymmetry (displayed as delta, e.g. RHS elongation – LHS elongation):

- Corner Angle: *PCL asymmetry was most sensitive* to this parameter, with PCL delta increasing between values of 0 degree to 30 deg before falling for higher angles. ACL elongation was found to be generally more severe for LHS impacts for corner angles between 0-35 with the RHS only being worse at the steepest corner angles. This behaviour generally matching previous understanding of the injury mechanics.
- PCL and ACL asymmetry reduces with increasing z height of the vehicle, driven by reduced bending of the legform upon impact due to engagement of the upper leg. This was also the case for MCL injury
- Nose angle was largely inconsequential to any of the cruciate ligament injuries and provided limited influence when compared to the other parameters in the DoE.

The global sensitivities analysis (GSA) from the metamodel is shown in Figure 12 below, demonstrating the respective influence of each vehicle parameter on ligament injury.

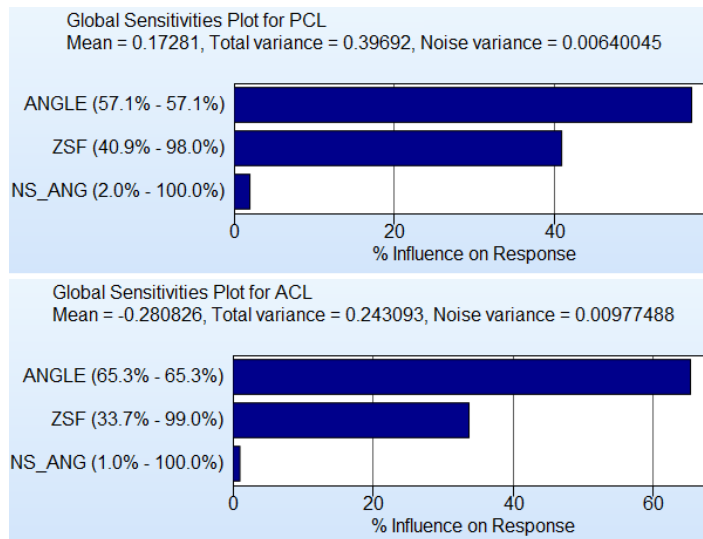


Figure 12 – PCL and ACL Global Sensitivity Analysis

Impactor Design of Experiments

Following on from the vehicle impactor study, a further study was undertaken with the Flex-PLI impactor to improve the understanding of impactor sensitivities on injury extent. This investigation reviewed rotations about the y and z directions, using the limits of UN ECE R127 to define the bounds of the design space. UN ECE R127 permits rotation to deviate from nominal by $\pm 2.5^\circ$ and $\pm 5.0^\circ$ respectively [1] (Figure 13).

A selection of 12 vehicle morphologies were chosen, based on the previous study results, as the basis for the impactor study. These morphologies represented points from across the original design space, with some chosen as the exacerbated the ligament asymmetries by the largest extent.

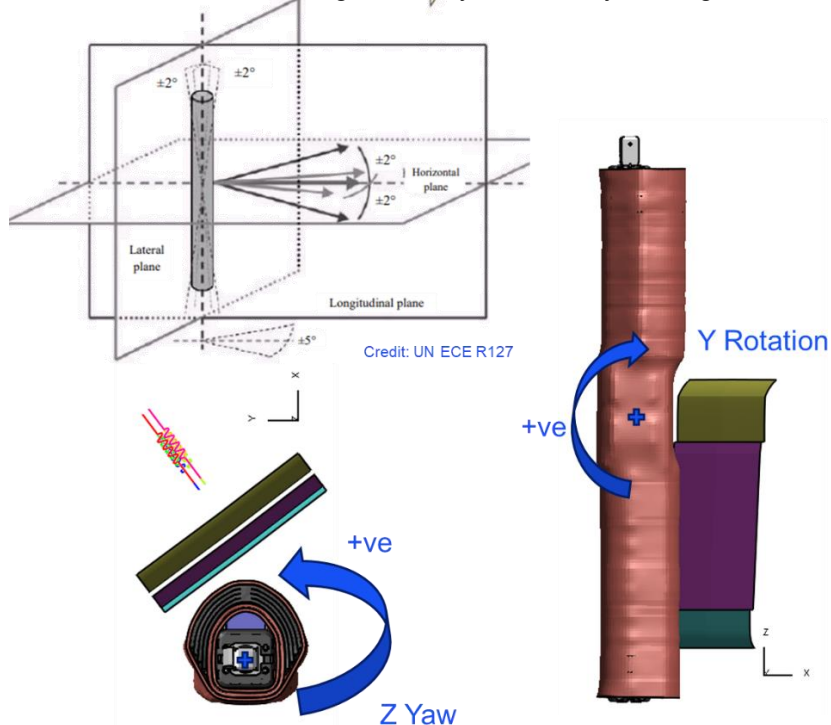


Figure 13 – UN ECE R127 Impactor rotation limits with rotation conventions applied for the study

Once again, a RHS and LHS simulation was ran for the 12 vehicle morphologies for both rotations and combinations of y and z. The dataset was analysed in LS-OPT, extracting linear correlation factors for each rotation and vehicle morphology, the results shown in Table 3.

Table 3 – Linear Correlations of ligament deltas for impactor studies

			Linear Correlation %			
Vehicle			Y Rotation		Z Rotation	
Angle	ZSF	Nose	PCL Delta	ACL Delta	PCL Delta	ACL Delta
5	1.33	45	0	38	-15	-88
15	1	0	0	5	-91	-86
25	1.33	60	13	41	-91	-74
37	1	20	11	9	-93	89
15	1.33	45	-19	0	-87	-90
25	1	0	5	-1	-99	-75
25	1.33	30	52	23	-78	-55
35	1	60	8	-9	-96	-16
35	2	45	-56	-19	33	54
45	1	0	12	-6	96	12
45	1.66	15	18	41	63	52
45	1.66	45	44	13	-53	63

Z rotation was found to be more influential to cruciate ligament injury than y rotation. A strong negative correlation was highlighted for PCL delta for morphologies that already demonstrate asymmetric injury behaviour. This indicated that the asymmetry between RHS and LHS *increases* as z impactor rotates clockwise, towards the vehicle. Certain morphologies (such as 37-1-20) were subject to noisier data pairs, which drive some anomalous correlation coefficients which warrant further investigation. For taller morphologies and higher corner angles, the correlation behaviour deviates from aforementioned trend.

Taking point 25-1.33-60 as an example, Figure 14 shows PCL injuries. The RHS is the worse side for injury with asymmetry greatest at negative z angles (clockwise), when impactor is rotated towards vehicle, increasing the tibial engagement with the vehicle. The greatest spread between elongations amount to 3.1mm right to left (red solid to red dashed).

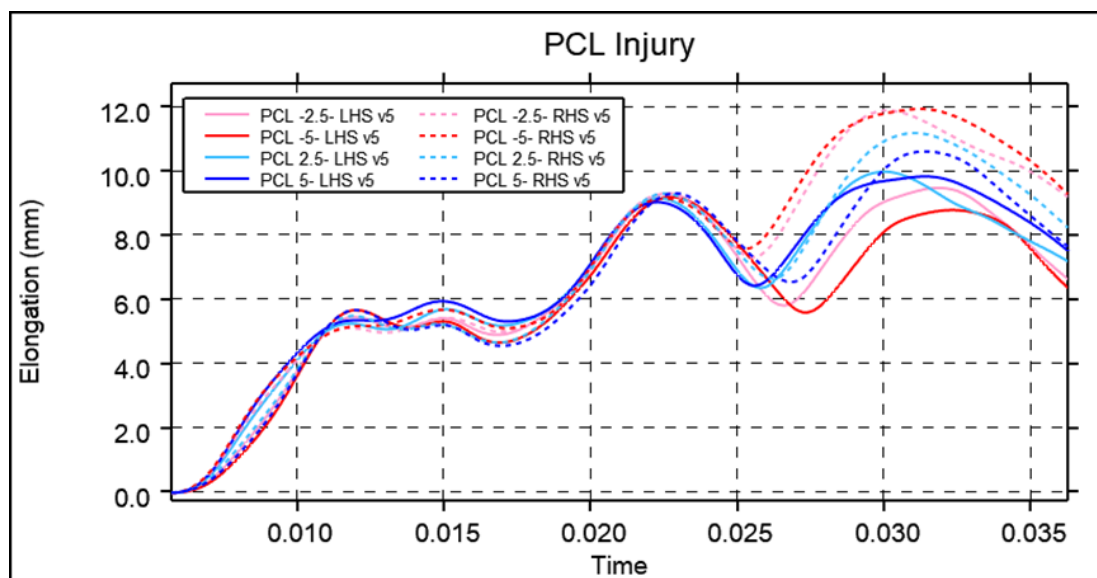


Figure 14 – PCL elongation for different rotation permutations (RHS dashed lines)

For ACL (Figure 15) injury LHS is worse case. Asymmetry is greatest at positive z angles (blue lines). This is when impactor is rotated away from vehicle. For ACL injuries, the greatest spread between elongations amount to 2.7mm right to left.

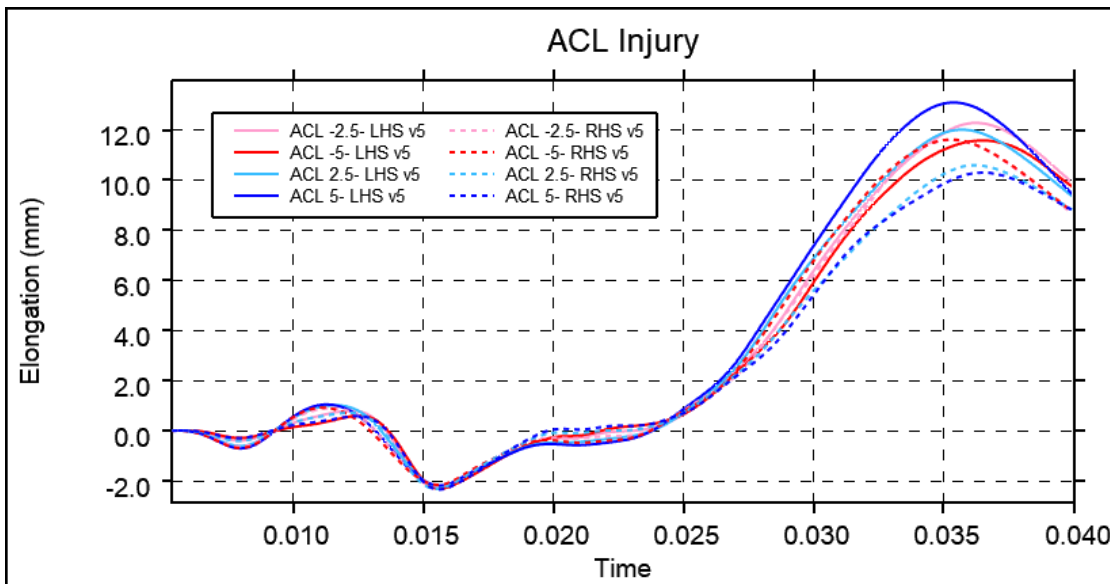


Figure 15 – ACL elongation for different rotation permutations (RHS dashed lines)

For the models experiencing the largest injury, the previously described mechanisms for exacerbated elongation are clearly demonstrated in the deformed shape (Figure 16).

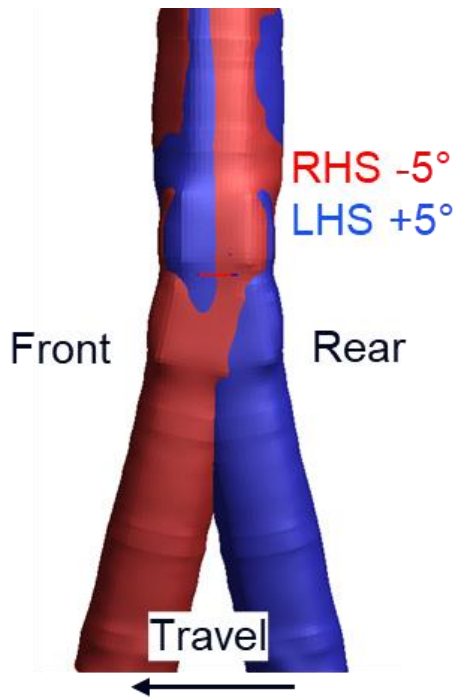


Figure 16 – Comparison of the most injury provoking rotations applied for a RHS and LHS impact that increase PCL and ACL injury respectively

This sensitivity to impactor z rotation highlights an aspect for safety specialists to be aware of when performing analysis for future vehicles; ensuring injuries remain within acceptable limits when applying these allowable rotations as worst-case scenarios.

aPLI Studies

Having assessed the sensitivity of Flex-PLI, a further study was conducted using the Humanetics aPLI impactor (v1.2) to infer whether this impactor was subject to the same extent of ligament sensitivity. The aPLI impactor has been adopted by various NCAP protocols since 2022, seen as an improvement in fidelity from Flex PLI, due to the inclusion of the upper body mass (Figure 17), which dramatically changes the kinematics of the aPLI impactor in comparison. This is in addition to a redesigned knee region, with updated flesh to bone distribution, new ligament routing and reshaping of the femoral condyle [3].



Figure 17 – View of both Humanetics aPLI (v1.2) and Flex-PLI (v1.5.1) ATD impactors, upper body mass and differing knee construction can be visualised compared to Flex PLI

This aPLI investigation uses the same vehicle morphologies identified in prior Flex PLI impactor studies in addition to the same impactor rotations. This particular investigation covered up to 95 sample pairs across the range of vehicle morphologies and different impactor y and z angles, *finding no significant variation between the RHS and LHS of the vehicle submodel*. Reviewing PCL, 85 of the 95 pairs were within 5% for the extent of elongation. Figure 18 and Figure 19 highlight how the LHS and RHS demonstrate far less variability than the Flex PLI impactor.

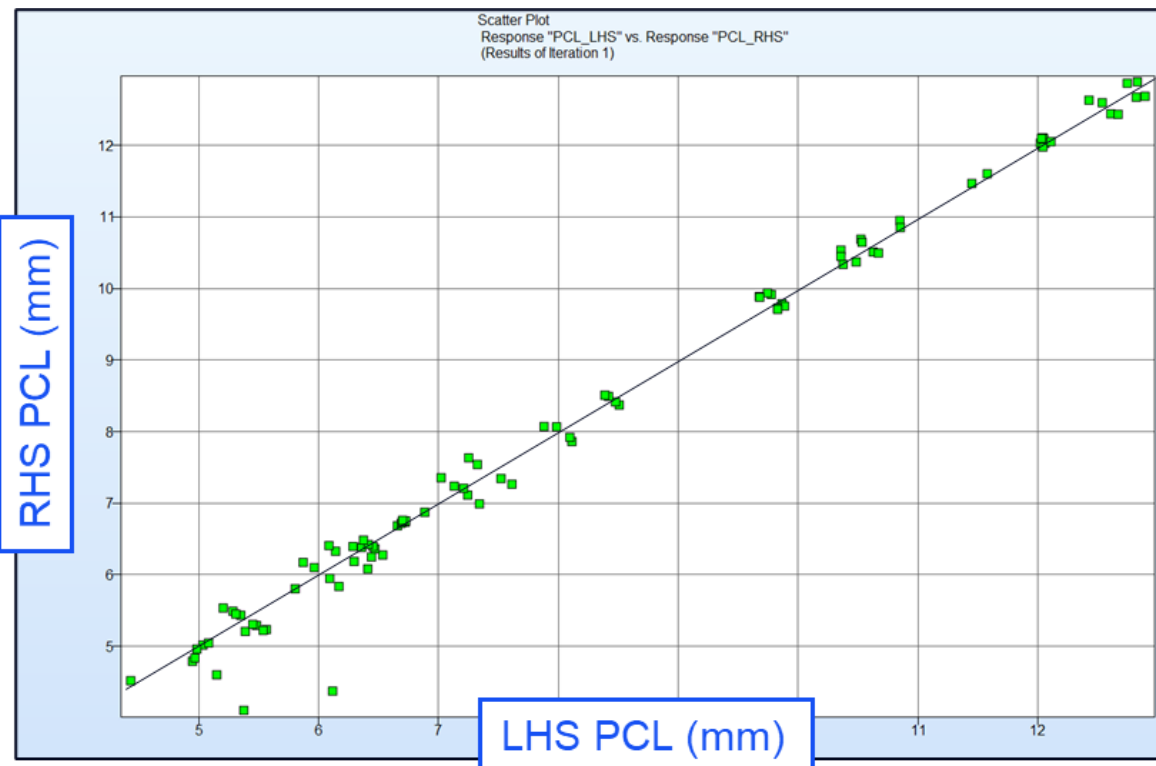


Figure 18 – LS-OPT Scatter plot of PCL injury across LHS and RHS.

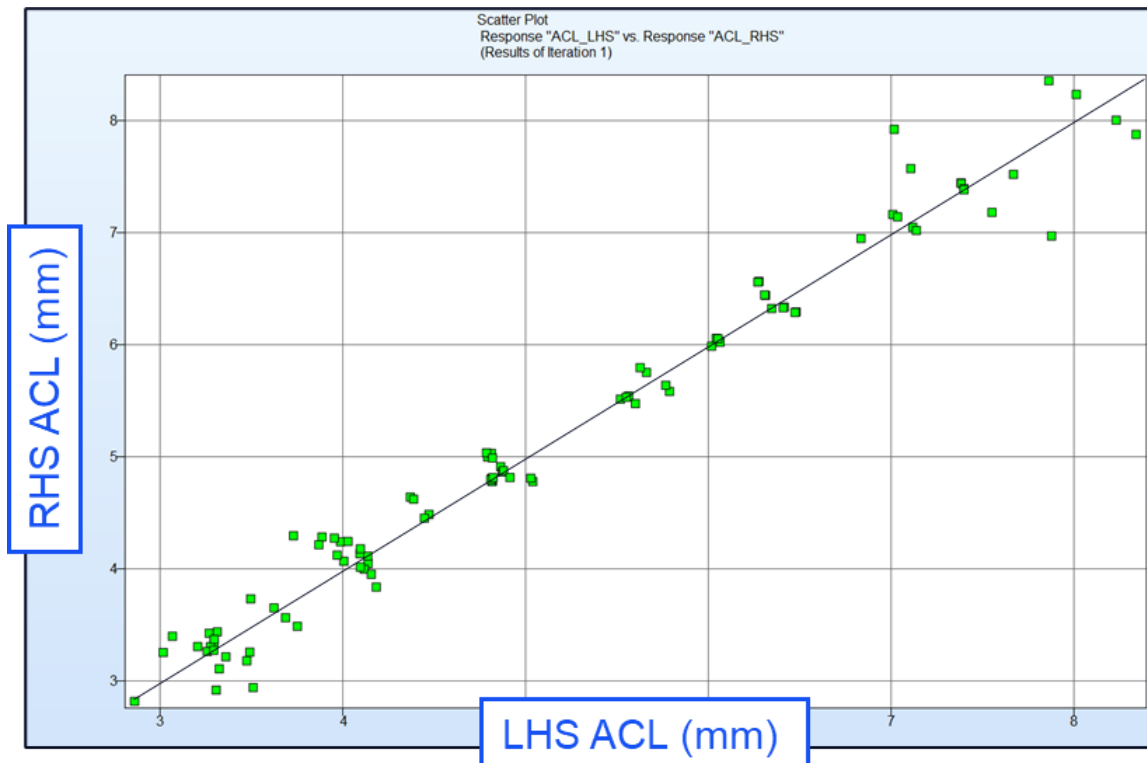


Figure 19 – LS-OPT Scatter plot of ACL injury across LHS and RHS. ACL injury demonstrating slightly higher variability than PCL

Further investigation is required to establish the exact mechanisms that cause lack of ligament sensitivity, whether it is entirely associated the addition upper body mass or another mechanism related to the updated construction of aPLI and knee compartment.

Human Body Model Studies

As a final investigation, the THUMS AM50 human body model, was used with the original full vehicle model to establish whether the leg hyperextension or increased PCL injury was observable during impact with the HBM. The HBM was placed relative to the vehicle so that the right knee aligned with the vehicle at the same y location as the ATD impactors for a RHS and LHS impact (Figure 20).

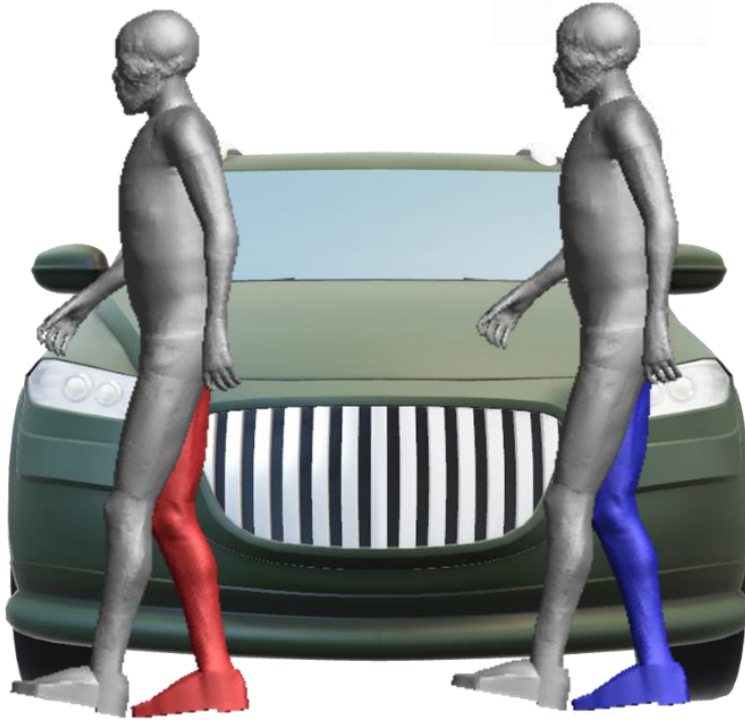


Figure 20 – HBM Impact (illustrative vehicle)

Unfortunately, this initial assessment with THUMS proved to be inconclusive. The peak ACL and PCL elongations are higher for the RHS impact compared to the LHS; however, the mechanism of injury is very different to what the ATD impactors exhibit. As Figure 21 demonstrates, the THUMS injuries are driven by significant tibial torsion, resulting in a pedestrian with a foot rotated in a highly severe manner.

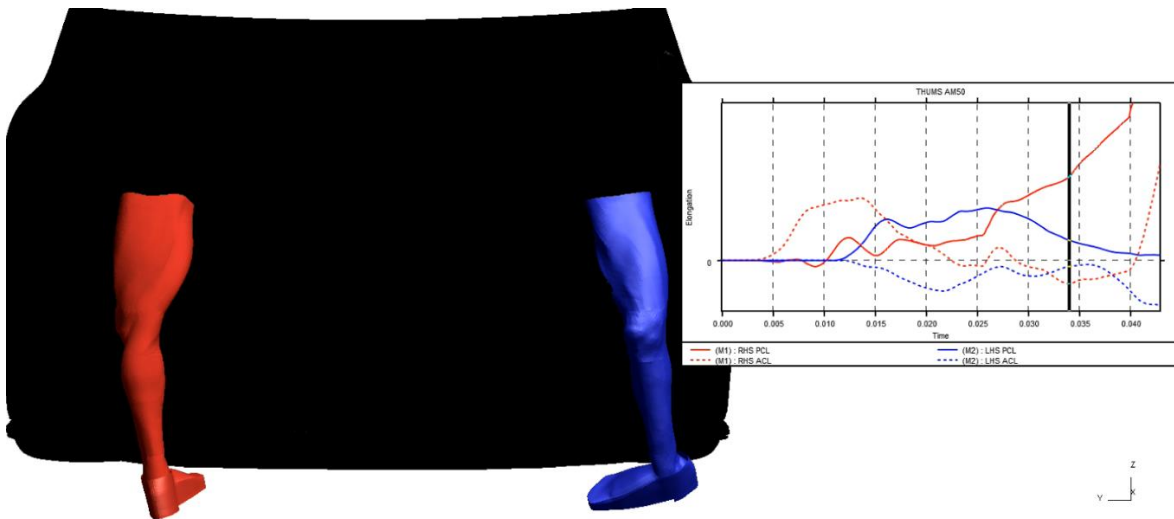


Figure 21 – RHS injuries driven by significant tibial torsion

Conclusion

This paper has explored the causation of pedestrian ATD ligament injury asymmetry in a sports vehicle physical test using LS-DYNA. The mechanisms of asymmetric ligament injuries were understood through review of biomechanics and evaluation of the Flex-PLI impactor during impact.

A submodel was developed and validated to a full vehicle FE model, subsequently being parameterised to evaluate the injury sensitivity across a range of vehicle morphologies in an initial study. This study found that corner angle and bumper height were the most influential parameters in inducing ligament asymmetry for both PCL and ACL. The outcomes of this study found that RHS impacts had a bias for increase PCL injury compared to the LHS. Conversely, ACL tended to be worse on the LHS.

A second study was conducted, using a subset of points from the previous study, evaluating the allowable rotations in the y and z axis for the impactor in the UN ECE R127 test protocol. Findings from this study identified that z axis rotation was most influential for cruciate ligament elongation. For the PCL, the RHS of the vehicle develops the worse case elongation, with rotation of the impactor towards the car increasing the amount of ligament injury. For ACL, the LHS of the car again is worst-case for elongation. Rotation of the impactor away from the vehicle worsened the injury.

Further studies using an aPLI impactor and THUMs HBMs were conducted to determine whether this asymmetric phenomena also appears. For aPLI, limited variability was detected for ligament injury between either side of the car, this likely due to the differing construction and behaviour of the aPLI impactor compared to Flex-PLI. The assessment using THUMs HBMs was deemed to be inconclusive due to the mechanism that the elongation was achieved.

Recommendations

Based upon the studies conducted in this paper, the authors recommend that for low vehicles, additional analyses for 'worst-case impacts' should be conducted, these being +/- 5-degree impactor yaw sensitivities at the extremities of the vehicle. Additionally, both vehicle sides should be routinely analysed, since RHS was observed to be worse for PCL and LHS worse for ACL when using a right leg impactor. The identified ligament phenomenon was especially pronounced for vehicles which bumper heights < 700mm, where the upper leg is not supported by the vehicle, and for corner angles between 15-35°.

Acknowledgements

The authors would like to thank Humanetics, who have generously supported this study, providing their time and access to leg impactor models.

References

[1] United Nations Economic Commission for Europe (UNECE), *Regulation No. 127: Uniform provisions concerning the approval of motor vehicles with regard to their pedestrian safety performance*, E/ECE/324/Rev.2/Add.126/Rev.3, Geneva, Switzerland, March 27, 2025.

[2] T. Isshiki, J. Antona-Makoshi, A. Konosu, and Y. Takahashi, "Consolidated Technical Specifications for the Advanced Pedestrian Legform Impactor (aPLI)," in *Proc. IRCOBI Conf.*, Athens, Greece, 2018, Paper No. IRC-18-42

[3] Humanetics Innovative Solutions, Inc., *API SBL-B Finite Element Model Version 1.2 Technical Report User's Manual*, Southfield, MI, [2022]

[4] Humanetics Innovative Solutions, Inc., *Flex PLI GTR REGULATED Version 1.5.1 LS-DYNA Finite Element Model User's Manual and Documentation*, Southfield, MI, [2021]

[5] LS-OPT® User's Manual, 7th ed., Livermore Software Technology Corporation, Livermore, CA, USA, 2020. [Online]. Available: <https://www.lsoptsupport.com/documents/manuals>

[6] LS-DYNA® Keyword User's Manual, Vol. I, R13, Livermore Software Technology, an Ansys Company, Livermore, CA, USA, Sep. 2021. [Online]. Available: <https://lsdyna.ansys.com/wp-content/uploads/2025/02/LS-DYNAManaulVolume/R13.pdf>